The Electrochemical Society
Advancing solid state & electrochemical science & technology

Modelling Solvent Consumption from SEI Layer Growth in Lithium-Ion Batteries

View the article online for updates and enhancements.

Modelling Solvent Consumption from SEI Layer Growth in Lithium-Ion Batteries

Ruihe Li,[1,2] Simon O'Kane,[1,2] Monica Marinescu,[1,2] and Gregory J Offer[1,2,*,z]

[1]*Department of Mechanical Engineering, Imperial College London, United Kingdom*
[2]*The Faraday Institution, United Kingdom*

Predicting lithium-ion battery (LIB) lifetime is one of the most important challenges holding back the electrification of vehicles, aviation, and the grid. The continuous growth of the solid-electrolyte interface (SEI) is widely accepted as the dominant degradation mechanism for LIBs. SEI growth consumes cyclable lithium and leads to capacity fade and power fade via several pathways. However, SEI growth also consumes electrolyte solvent and may lead to electrolyte dry-out, which has only been modelled in a few papers. These papers showed that the electrolyte dry-out induced a positive feedback loop between loss of active material (LAM) and SEI growth due to the increased interfacial current density, which resulted in capacity drop. This work, however, shows a negative feedback loop between LAM and SEI growth due to the reduced solvent concentration (in our case, EC), which slows down SEI growth. We also show that adding extra electrolyte into LIBs at the beginning of life can greatly improve their service life. This study provides new insights into the degradation of LIBs and a tool for cell developers to design longer lasting batteries.
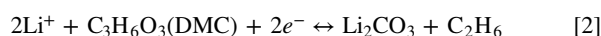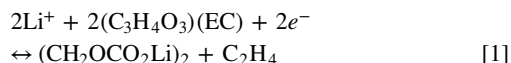
Lithium-ion batteries (LIBs) are widely used in portable electronic devices, electric vehicles, and grid storage. However, the degradation of LIBs, causing power and capacity fade, is a significant problem for all applications. Degradation of LIBs is caused by a significant number of state dependent and tightly coupled mechanisms.[1] Understanding these mechanisms and modelling them can give cell designers and users useful tools to alleviate the degradation of LIBs from the perspective of both manufacture and management during use.

The physics-based battery life models in literature to date have predominantly focussed on solid-electrolyte interface (SEI) layer growth,[2,3] lithium plating,[4,5] dissolution of the positive electrode,[6,7] and crack growth.[8,9] Among these, many researchers agree that SEI layer growth is the dominating degradation mechanism in most applications, especially at the beginning-of-life.[10–12] The SEI layer forms on the negative electrode particle surfaces as a solvent or additive decomposition product from reaction with cyclable lithium, initially during the formation cycle and subsequent gradual growth as the cell ages.[11,13,14] One of the few conditions that slows down SEI growth is low temperature,[11,15] but this can cause other degradation mechanisms to dominate, such as lithium plating and/or particle cracking. An accurate physics-based battery life model should consider as many direct or indirect effects of SEI growth as possible. To achieve this, we start from the following two widely adopted reactions describing SEI growth:[4]

$$2Li^+ + 2(C_3H_4O_3)(EC) + 2e^-$$
$$\leftrightarrow (CH_2OCO_2Li)_2 + C_2H_4 \qquad [1]$$

$$2Li^+ + C_3H_6O_3(DMC) + 2e^- \leftrightarrow Li_2CO_3 + C_2H_6 \qquad [2]$$

The reactions in Eqs. 1 and 2 involve

1. the consumption of lithium-ions;
2. the consumption of solvent components, i.e., EC and DMC;
3. the generation of the porous $((CH_2OCO_2Li)_2)$ and dense (Li_2CO_3) components, and therefore thickening of the SEI layers;
4. the generation of two gases.

Among these, the consumption of lithium ions, known as loss of lithium inventory (LLI), has been well addressed in previous works.[2,4,5,16–19] LLI causes capacity loss and therefore models including this consequence can be fitted to experimental capacity fade reasonably well. The thickening of the SEI layers also causes a porosity reduction and an increased impedance in the negative electrode.[2,4,5,18,19] However, the consumption of solvent components and generation of gases are regularly omitted. In a recent work of Atalay et al.[4] on modelling the two-layer SEI growth, they included solvent consumption by reducing the volume fraction of solvent components. However, they maintained a crucial assumption made in all previous papers[2,5,18,19] that the total pore volume always equals the total electrolyte volume. Since the porosity change in many of these models is normally induced by SEI thickening, this assumption means that the increased volume due to SEI thickening always equals the decreased volume of electrolyte due to solvent consumption, which is almost impossible. For example, for the reaction in Eq. 1, the consumption of 1 mol DMC corresponds to the generation of 1 mol Li_2CO_3. If we ignore the gas phase and the solute-volume effects,[20] the decreased volume of electrolyte due to solvent consumption would be 110 ml, while the decreased pore volume due to SEI thickening would be only 35 ml. That means part of the pores will be filled by nothing, i.e., part of the active jelly roll (JR) region will dry out, unless these pores can be replenished by extra electrolyte stored outside the JR but inside the cell package. It is normal that extra electrolyte is added into cells during manufacturing, to ensure good wettability and better performance.[21] If any remains after formation, the empty pore volume can be replenished by the extra electrolytes outside the Jr However, the replenishment will change the concentration of lithium-ions and solvent components, which also needs to be considered as such concentration changes significantly impact both the main and side reaction rates.[2–5,18,19]

Electrolyte dry-out is a phenomenon that has been experimentally observed but seldom been modelled.[22–24] Ren et al.[24] cycled a 24 Ah pouch cell at 2C/25 °C until 80% SOH and found that the disassembled cell exhibited obvious dry-out near the JR edges. The negative electrode also contained some lithium metal as detected by nuclear magnetic resonance (NMR), indicating the electrolyte dry-out was accompanied by lithium plating. One straightforward effect of electrolyte dry-out is that the dried electrode area becomes inactive, subjecting the remaining adjacent electrode area to higher current density and therefore increasing the possibility of lithium plating.[23] Regarding modelling, Park et al.[25] predicted capacity drop with an empirical model for electrolyte depletion by multiplying the electrolyte volume fraction by a

modified step function. However, the provided step function is a purely empirical fifth order polynomial and therefore could be an example of over-fitting. Kupper et al.[26] introduced two parameters to describe electrolyte depletion, namely the "activity," which is the ratio between active graphite and total graphite; and the "saturation," which is the ratio between electrolyte volume and summation of electrolyte volume and gas volume. This is based on the percolation theory that the gas produced during SEI reaction would deactivate part of the graphite electrode and therefore induce LAM in the negative electrode. To capture capacity drop observed in experiments, a nonlinear relationship between the activity and the saturation is assumed. Fang et al.[27] introduced a drying coefficient, defined as the ratio between the volume of the remaining electrolyte and the total pore volume in the Jr Upon dry-out, this ratio would decrease three key parameters in the model, namely the interfacial surface area, the electrolyte volume fraction and active material volume fraction. The resulting positive feedback loop between LAM and SEI growth would then predict capacity drop as well. Kupper et al.[26] acknowledged the existence of a competing negative feedback mechanism, in which solvent consumption reduces the rate of further SEI formation. However, they found the positive feedback to be stronger, leading to capacity drop. In this work, positive feedback means that the different degradation mechanisms cause each other to accelerate and trigger capacity drop, whereas negative feedback means the opposite.

All three works on modelling electrolyte depletion can predict the capacity retention curves well. However, two critical points have been ignored. If there is excess electrolyte outside the JR but inside the LIB package, the excess electrolyte will enter the JR to fill the gap caused by solvent consumption. Such electrolyte mixing will change the concentration of solvent and Li$^+$ in the electrolyte in the JR, influencing the electrolyte conductivity and diffusivity. Even if there is no excess electrolyte, solvent consumption increases the concentration of Li$^+$ relative to solvent, which also changes the conductivity and diffusivity. It remains unclear how the initial electrolyte volume in fresh cells will affect the cycle life of LIBs.

Therefore, we aim to fill the above research gaps by considering, for the first time, the effects of change in Li$^+$:solvent ratio and excess electrolyte on the degradation behaviour of LIBs. This paper is organized as follows. We first introduce the physics-based battery life model which contains a Doyle-Fuller-Newman (DFN) model, a diffusion-limited SEI model and a novel solvent consumption model. Then, the ageing mechanisms of this model are analysed and correlated to the solvent consumption and possible dry-out. Finally, the effects of solvent consumption on the lithium-ion and solvent concentration and resulting electrolyte transportation properties are evaluated.

Model Description

To simulate the effect of electrolyte dry-out on the performance of LIBs, this study establishes a physics-based battery life model which couples a novel solvent consumption model with the classical Doyle-Fuller-Newman (DFN) model and the diffusion-limited SEI model.

DFN model with diffusion-limited SEI growth model.—The DFN model describes the main reaction of LIBs, i.e., lithium (de-)intercalation. The diffusion limited SEI model captures the SEI growth process, for which the reaction rate is limited by the solvent transportation through the outer SEI layer.

The DFN model has been widely used in modelling the electrochemical response of LIBs.[28] It consists of two charge conservation equations, two mass conservation equations, and one kinetic equation, as presented in Table I. More comprehensive introduction of this model can be found in Refs. 29, 30.

One variable which directly connects the DFN model and the SEI model is the volumetric current density. The total current density in

the charge conservation for electrodes is

$$j_k^{\text{total}} = \begin{cases} j_k^{\text{int}} + j_{\text{SEI}}, & k = n \\ j_k^{\text{int}}, & k = p \end{cases} \quad [3]$$

This study utilizes the diffusion limited SEI growth model. It is assumed that the SEI reaction happens at the interface between the inner and outer SEI layers.[3] Therefore, the current density of the SEI reaction in Eq. 1 is[3,32]

$$j_{\text{SEI}} = -F \cdot a_n \cdot D_{\text{EC}}^{\text{SEI,out}} \cdot c_{\text{EC}} / \delta_{\text{SEI,out}} \quad [4]$$

where F and a_n are the Faraday constant and the specific surface area, respectively. For spherical particles $a_n = 3\varepsilon_n/R_n$, where R_n is the radius of the negative electrode particles. $D_{\text{EC}}^{\text{SEI,out}}$ is the diffusivity of the solvent (in this case, EC) in the outer SEI layer, c_{EC} is the EC concentration and $\delta_{\text{SEI,out}}$ is the thickness of outer SEI layer. Note that both the EC concentration and lithium-ion concentration in this work are calculated by moles over the electrolyte volume in the jelly roll.

Here we assume that the SEI consists of two layers and that reaction occurs at the interface between the inner and outer layers. These two layers share the current density in Eq. 1 as follows:[3]

$$j_{\text{SEI,in}} = \alpha \cdot j_{\text{SEI}} \quad [5]$$

$$j_{\text{SEI,out}} = (1 - \alpha) \cdot j_{\text{SEI}} \quad [6]$$

where α is a coefficient and $j_{\text{SEI,in}}$ and $j_{\text{SEI,out}}$ are the current densities of the inner and outer SEI layers, respectively. If $\alpha = 0.5$, the inner and outer SEI layers will growth at the same rate.

We assume the SEI reaction to be Eq. 1, which means that the stoichiometric ratio of Li$^+$, EC, electrons and SEI product is 2:2:2:1. With the current passing through, the total thickness of SEI layer will increase as follows:[2]

$$\frac{d\delta_{\text{SEI}}}{dt} = -\frac{j_{\text{SEI}}}{2a_n F} \cdot \frac{M_{\text{SEI}}}{\rho_{\text{SEI}}} \quad [7]$$

where M_{SEI} and ρ_{SEI} are the molar mass and density of SEI layers, respectively.

The thickening of the SEI layers will have two direct effects:

1) decrease the porosity of the electrode:[5]

$$\frac{d\varepsilon_n}{dt} = -a_n \cdot \frac{d\delta_{\text{SEI}}}{dt} \quad [8]$$

2) increase the resistance of SEI films, which further increases the SEI overpotential:[3]

$$\eta_{\text{SEI}} = \frac{j_n^{\text{tot}} \delta_{\text{SEI}}}{a_n \sigma_{\text{SEI}}} \quad [9]$$

where ε_n and σ_{SEI} are the conductivity of the SEI layers and the porosity of the negative electrodes, respectively.

The initial conditions for δ_{SEI} and ε_n are:

$$\delta_{\text{SEI}}|_{t=0} = \delta_{\text{SEI}}^0 \quad [10]$$

$$\varepsilon_n|_{t=0} = \varepsilon_n^0 \quad [11]$$

Solvent consumption model.—The solvent consumption model aims to describe both direct and indirect effects of SEI growth. We will construct this model as follows. First, we will introduce the new independent variables describing the electrolyte volume. Second, we

Table I. Equation of P2D model used in the simulations.[5,31]

Description	Equation	Boundary condition
	Electrode	
Mass conservation	$\frac{\partial c_{s,k}}{\partial t} = \frac{1}{r^2}\frac{\partial}{\partial r}\left(r^2 D_{s,k}\frac{\partial c_{s,k}}{\partial r}\right)$	$\frac{\partial c_{s,k}}{\partial r}\Big|_{r=0}=0,\ -D_{s,k}\frac{\partial c_{s,k}}{\partial r}\Big|_{r=R_k}=\frac{j_k^{tot}}{a_k F}$
Charge conservation	$\frac{\partial}{\partial x}\left(\sigma_{s,k}\frac{\partial \phi_{s,k}}{\partial x}\right)=j_k^{tot}$	$-\sigma_{s,n}\frac{\partial \phi_{s,n}}{\partial x}\Big|_{x=0}=-\sigma_{s,p}\frac{\partial \phi_{s,p}}{\partial x}\Big|_{x=L}=i_{app}$
		$-\sigma_{s,n}\frac{\partial \phi_{s,n}}{\partial x}\Big|_{x=L_n}=-\sigma_{s,p}\frac{\partial \phi_{s,p}}{\partial x}\to\frac{\partial \phi_{s,p}}{\partial x}\Big|_{x=L-L_p}=0$
	Electrolyte	
Mass conservation	$\frac{\partial \varepsilon_k c_{e,k}}{\partial t}=\begin{cases}\frac{\partial}{\partial x}\left(\varepsilon_k^b D_e\frac{\partial c_{e,k}}{\partial x}\right)+(1-t^+)\frac{j_k^{tot}}{F},\ k=n,p\\ \frac{\partial}{\partial x}\left(\varepsilon_k^b D_e\frac{\partial c_{e,k}}{\partial x}\right),\ k=s\end{cases}$	$\frac{\partial c_{e,n}}{\partial x}\Big|_{x=0}=\frac{\partial c_{e,p}}{\partial x}\Big|_{x=L}=0$
Charge conservation	$\frac{\partial}{\partial x}\left(\varepsilon_k^b \sigma_e\left(\frac{\partial \phi_{e,k}}{\partial x}-\frac{2(1-t^+)RT}{F}\frac{\partial \log c_{e,k}}{\partial x}\right)\right)=-j_k^{tot}$	$\frac{\partial \phi_{e,n}}{\partial x}\Big|_{x=0}=\frac{\partial \phi_{e,p}}{\partial x}\Big|_{x=L}=0$
	Reaction kinetics	
Butler-Volmer	$j_k^{int}=\begin{cases}a_k j_{0,k}^{int}\sinh\left(\frac{1}{2}\frac{RT}{F}\eta_k^{int}\right),\ k\in\{n,p\},\\ 0,\ k=s.\end{cases}$	
Exchange current	$j_{0,k}^{int}=k_k\sqrt{c_{e,k}c_{s,k}(r)(c_{s,k}^{max}-c_{s,k}(r))}\big|_{r=R_k}$	
Overpotential	$\eta_k^{int}=\begin{cases}\phi_{s,n}-\phi_{e,n}-U_{e,n}(c_{s,n}\big|_{r=R_n})-\eta_{SEI},\ k=n,\\ \phi_{s,p}-\phi_{e,p}-U_{e,p}(c_{s,p}\big|_{r=R_p}),\ k=p.\end{cases}$	
	Initial conditions	
Initial conditions	$c_{s,k}=c_{k0}\ (k=n,p),\ c_{e,k}=c_{e0}\ (k=n,s,p)$	
	Terminal voltage	
Terminal voltage	$V=\phi_{s,p}\big|_{x=L}-\phi_{s,n}\big|_{x=0}$	

will derive the equations for the solvent consumption and replenishment, followed by the description of electrolyte dry-out. Finally, we will discuss the effect of the solvent consumption and replenishment on the lithium ion and solvent (in our case, EC) concentration.

New independent variable.—To begin with, we assume that fresh LIBs contain extra electrolyte outside the JR but inside the cell package. We call this extra electrolyte the reservoir, with the volume being V_e^{res}. The total electrolyte volume inside the cell package is therefore

$$V_e^{cell}=V_e^{res}+V_e^{JR} \quad [12]$$

where V_e^{JR} is the electrolyte volume inside the Jr Both V_e^{res} and V_e^{JR} are new independent variables compared to previous studies, with the initial conditions being

$$V_e^{res}\big|_{t=0}=V_e^{res,0} \quad [13]$$

$$V_e^{JR}\big|_{t=0}=V_e^{JR,0}=A_{cell}^0(L_n\varepsilon_n^0+L_s\varepsilon_s^0+L_p\varepsilon_p^0) \quad [14]$$

where L_n, L_s, and L_p are the thicknesses of the negative electrode, separator, and positive electrode respectively. The thicknesses of the three components will remain the same for aged cells and therefore no ^{0} superscripts are added. ε_n^0, ε_s^0, and ε_p^0 are the initial porosities of the negative electrode, separator, and positive electrode, respectively. A_{cell}^0 is the initial area of the cell, which is equal to the product of the initial electrode length and width.

Solvent consumption, replenishment and dry out.—Liquid electrolytes, which fill the pores of the negative electrodes, positive electrodes, and separators of jelly rolls, normally consist of aqueous solvents such as EC, DMC, EMC, etc., which are mixed with LiPF$_6$.[14,33] A schematic of a negative electrode filled with electrolyte is shown in Figs. 1d–1f. The red boundary in Figs. 1d–1f shows the total pore volume of the JR;

the coloured blocks inside the red boundary indicate the electrolyte volume. Note that these coloured blocks are separated in Fig. 1 just for clarity; in real electrolytes in LIBs, different solvents are mixed. Our second assumption is that these solvents retain their initial volume before being mixed in the composite electrode. Meanwhile, we also assume the LiPF$_6$ does not contribute to the volume of the electrolyte; and that only EC is consumed during cell ageing.

Now we consider electrolyte consumption in the negative electrode due to the SEI reaction 1. We start from the initial stage (Fig. 1d, moment t) when all the pores in the JR are filled with electrolyte. After a certain period dt, some EC is consumed together with some porosity (Fig. 1e, moment $t+dt^-$). The decreased EC volume will be equal to the decreased electrolyte volume

$$dV_e^{JR}=dV_{EC}=dn_{EC}\cdot\frac{M_{EC}}{\rho_{EC}} \quad [15]$$

where dn_{EC} is the number of moles of EC consumed within a period dt and M_{EC} and ρ_{EC} are the molar mass and density of EC, respectively.

Besides, the decrease in pore volume due to the reaction in Eq. 1 is

$$-dV_{pore}=dV_{SEI}=dn_{SEI}\cdot\frac{M_{SEI}}{\rho_{SEI}}=-\frac{dn_{EC}}{2}\cdot\frac{M_{SEI}}{\rho_{SEI}} \quad [16]$$

where dn_{SEI} is the number of moles of SEI (in this case, (CH$_2$OCO$_2$Li)$_2$) generated within a period dt.

The volume and thickness change of the SEI layers can be linked through[2,5]

$$d\delta_{SEI}=\frac{dn_{SEI}}{a_n A_{cell}L_n}\cdot\frac{M_{SEI}}{\rho_{SEI}} \quad [17]$$

In most previous works,[2,5,18,19] the volume changes of pores and electrolytes are automatically regarded as equal, because there is no
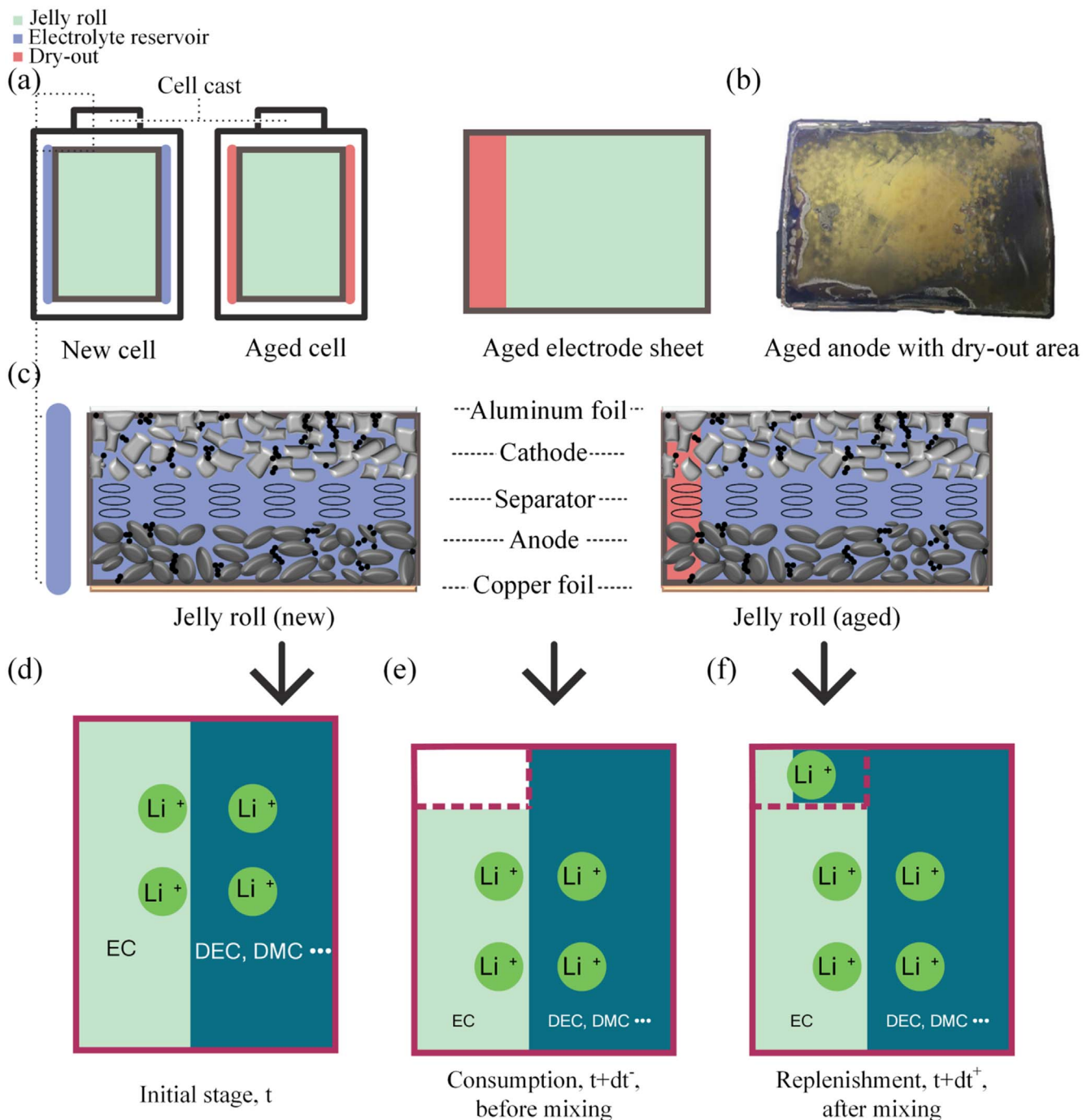
Figure 1. Illustration of solvent consumption in dry-out in LIB pouch cells. (a) Sketches of new and aged cells. (b) Aged anode with dry-out area. Reproduced from [1]. (c) Schematic of how dry-out deactivate some electrode materials in a jelly roll. (d) Schematic of how electrolyte from the reservoir mix with those in jelly roll.

independent variable for the electrolyte volume in the model. Such forced equilibrium means

$$\frac{M_{EC}}{\rho_{EC}} = \frac{1}{2} \cdot \frac{M_{SEI}}{\rho_{SEI}} \qquad [18]$$

However, 18 is wrong in most cases. For the reaction in Eq. 1, we have[4]

$$\frac{M_{EC}}{\rho_{EC}} > \frac{1}{2} \cdot \frac{M_{SEI}}{\rho_{SEI}} \qquad [19]$$

Therefore, we have

$$dV_e^{JR} < dV_{pore} = -dV_{SEI} < 0 \qquad [20]$$

$$V_e^{JR}|_{t+dt^-} < V_{pore}|_{t+dt^-} \qquad [21]$$

Eqs. 20 and 21 mean that the decreased volume due to electrolyte consumption is larger than the increased volume due to SEI formation, producing pores filled with nothing. Note that all these species are inside the Jr For LIBs with an electrolyte reservoir ($V_e^{res} > 0$), these empty pores inside the JR can be replenished by the

electrolyte in the reservoir due to hydrodynamics. We assume that the time needed for such replenishment, $dt^+ - dt^-$, is negligible compared to dt. Therefore, we have

$$dV_e^{res} = -dV_e^{add} = dV_e^{JR} - dV_{SEI} \qquad [22\text{-}1]$$

$$V_e^{JR}|_{t+dt^+} = V_e^{JR}|_{t+dt^-} + dV_e^{add} \qquad [23\text{-}1]$$

$$V_{pore}|_{t+dt^+} = V_{pore}|_{t+dt^-} \qquad [24\text{-}1]$$

Therefore

$$V_e^{JR}|_{t+dt^+} = V_{pore}|_{t+dt^+} \qquad [25\text{-}1]$$

For LIBs without an electrolyte reservoir ($V_e^{res} = 0$), we have

$$dV_e^{res} = dV_e^{add} = 0 \qquad [22\text{-}2]$$

$$V_e^{JR}|_{t+dt^+} = V_e^{JR}|_{t+dt^-} + 0 \qquad [23\text{-}2]$$

$$V_{pore}|_{t+dt^+} = V_{pore}|_{t+dt^-} \qquad [24\text{-}2]$$

Therefore

$$V_e^{JR}|_{t+dt^+} < V_{pore}|_{t+dt^+} \qquad [25\text{-}2]$$

In the case of $V_e^{res} = 0$, the newly formed empty pores will de-activate the active materials nearby as the ion transportation is no longer possible. To implement such a dry-out effect in the P2D model with minimal changes to the current equations, we simply shrink the electrode area by a dry-out ratio. This ratio is defined as the total electrolyte volume divided by the total pore volume inside the JRs

$$R_{dry}|_{t+dt} = \frac{V_e^{JR}|_{t+dt^+}}{V_{pore}|_{t+dt^+}} \qquad [26]$$

Then the electrode area becomes

$$A_{cell}|_{t+dt^+} = R_{dry}|_{t+dt} \cdot A_{cell}|_{t+dt^-} \qquad [27]$$

Lithium ion and EC concentration.—The concentration of lithium ions and solvents will change due to EC consumption, whether $V_e^{res} = 0$ or $V_e^{res} > 0$. Now we make our fifth assumption that the electrolyte in the reservoir has the same lithium ion and EC concentration as the initial JR (moment $t = 0$). We further assume that the added electrolyte changes the concentration of lithium ions in every location of the cell by the same ratio (Fig. 1f):

$$R_{Li^+} = \frac{c_{Li^+}(x, t + dt^+)}{c_{Li^+}(x, t + dt^-)} \qquad [28]$$

The total number of lithium ions in the cell must be conserved:

$$\int c_{Li^+}(x, t + dt^+) \cdot \varepsilon_n(t) dV_{JR}|_{t+dt^+}$$

$$= R_{Li^+} \int c_{Li^+}(x, t + dt^-) \cdot \varepsilon_n(t) dV_{JR}|_{t+dt^+}$$

$$= \int c_{Li^+}(x, t + dt^-) \cdot \varepsilon_n(t) dV_{JR}|_{t+dt^-} + c_{Li}^0 \cdot dV_e^{add} \qquad [29]$$

The ratio for lithium concentration change is therefore:

$$R_{Li^+} = \frac{\int c_{Li^+}(x, t + dt^-) \cdot \varepsilon_n(t) dV_{JR}|_{t+dt^-} + c_{Li}^0 \cdot dV_e^{add}}{\int c_{Li^+}(x, t + dt^-) \cdot \varepsilon_n(t) dV_{JR}| t + dt^+} \qquad [30]$$

We assume EC is homogenous across the electrode, i.e., the EC concentration is independent of location. Therefore:

$$c_{EC}(t + dt^+) = \frac{V_e(t) \cdot c_{EC}(t + dt^-) - dn_{EC} + c_{EC}^0 \cdot dV_{add}}{V_e(t + dt^-) - dV_e + dV_{add}} \qquad [31]$$

The ratio for EC concentration change is:

$$R_{EC} = \frac{c_{EC}(t + dt^+)}{c_{EC}(t + dt^-)} \qquad [32]$$

Instead of directly setting the volume of electrolyte in the reservoir as a variable, we define the ratio of initial extra electrolyte R_e^{res}:

$$R_e^{res} = V_e^{res,0}/V_e^{JR,0} \qquad [33]$$

where $V_e^{res,0}$ and $V_e^{JR,0}$ are the initial volume of the electrolyte reservoir and the electrolyte in the JR, respectively.

Model implementation.—The three models are implemented in the open-source package Python Battery Mathematical Modelling (PyBaMM).[34] The DFN model and diffusion-limited SEI growth model are two built-in models in PyBaMM. Table II shows the cycling protocol for the degradation modelling. Firstly, cells are cycled in a reference performance test (RPT) to evaluate the capacity retention, followed by the ageing test. The RPT and ageing tests are repeated 15 times. After that, another RPT is conducted to evaluate the final performance of the aged cells.

Adding another variable into a set of differential equations will increase the required computational resources and lower the speed. To implement the model with fewer computational resources and no change to PyBaMM, we do not add new differential equations of electrolyte variables. Instead, we update the model as EC is consumed using the three ratios (R_{dry}, R_{Li^+}, R_{EC}) defined in Eqs. 26, 30 and 32. The proposed update method is illustrated in Fig. 2. We first initialize the model with the parameters listed in Tables A·I and A·II. Then, the cells are cycled following the protocols in Table I inside PyBaMM. At the end of each RPT and

Table II. Cycling protocol for the degradation modeling.

Tests	Procedure	Repeated times
RPT test	(1) CC discharge at 0.1 C to 2.5 V	16
	(2) Rest for 6 h	
	(3) CC charge at 0.1 C to 4.2 V	
Ageing test	(1) CC discharge at 1 C to 2.5 V	15
	(2) CC charge at 0.3 C to 4.2 V	
	(3) CV charge at 4.2V until current $<$ 0.01 C	
	(4) Loop Step (1) to (3) for 78 times	

part of each ageing test, we stop the cycling and extract the cell status at the end of the previous cycle. Then, the electrode area is updated by R_{dry}, while the lithium concentration and bulk EC concentration are updated by R_{Li^+} and R_{EC}, respectively. The updated process is carried out outside PyBaMM, and the resulting status will act as an input for the further cycling. The detailed code can be found on GitHub (https://github.com/RuiheLi/PyBaMM/blob/SolventConsumption/examples/notebooks/Solvent%20consumption%20model%20-%20RHL%20-%20Imperial.ipynb).

The proposed update method should give similar results as adding new differential equations, since the electrolyte consumption process is a slow and long-term ageing process.[11] In order to justify the use of this method, we compare the results obtained by setting different update frequencies for the ageing tests in the Appendix. We run the simulation in a normal PC, with an Intel Core i7–6700 processor and 64GB RAM. We can run up to three scripts in Jupiter Notebook simultaneously, and each script takes about 2 h and 40 min to finish 1170 cycles on average.

Results and Discussion

Ageing mechanisms.—To quantify the effects of solvent consumption on the degradation behaviours of LIBs, we analyse the capacity retention, LLI, LAM, and resistance increase of cells with and without the solvent consumption model (Fig. 3). Note that the cells without solvent consumption can only be cycled for 1092 cycles because further cycling results in the local lithium-ion concentration in the electrolyte reaching zero in the model even though the average lithium-ion concentration increases. The discharge capacity in Fig. 3a is obtained from the 0.1C discharge process in each RPT.

In Fig. 3a, all the curves exhibit decelerating capacity fade as a result of the self-limiting SEI growth,[35] but with different degradation rates. The cell with 0% more electrolyte and the cell without solvent consumption both lost ~18% capacity after 1092 cycles. However, the cell with 0% more electrolyte degrades more quickly at the early stage and more slowly at the late stage, whereas the degradation rate of the cell without solvent consumption changes more slowly. This is because LAM occurs in the early ageing cycles in the cell with 0% more electrolyte due to the electrolyte dry-out, while the cell without solvent consumption has no LAM. Moreover, the LAM of the cell with 0% more electrolyte in Fig. 3c also has a decelerating trend with cycle number as it originates from the SEI driven electrolyte dry-out. Furthermore, the cell without solvent

consumption has more LLI due to SEI growth (Fig. 3b) and a larger resistance increase. The different degradation mechanisms of these two cells lead to the same capacity retention after 1092 cycles.

The cells with 6% and 9% more electrolyte retain more capacity than the other two cells in Fig. 3a. To be specific, the cell with 9% more electrolyte retains 89% capacity after 1170 cycles, because there is zero LAM throughout the ageing cycles and a smaller resistance increase. The cell with 6% more electrolyte initially behaves the same as the cell with 9% more electrolyte but deviates at the 390th cycle and retains 85% capacity after 1170 cycles. This deviation point at the 390th cycle also occurs in Figs. 3b–3d and marks the start of electrolyte dry-out.

Another interesting observation is that the LLI of different cells with solvent consumption (Fig. 3b) shows the opposite trend to the LAM (Fig. 3c). For example, the cell with 0% more electrolyte has lower LLI and higher LAM than the cell with 9% more electrolyte. One possible reason is that our model deactivates part of the electrode when dry-out occurs. Cells with fewer active electrode particles, i.e., more LAM, will therefore have less SEI formation and LLI.

To summarize, models not considering the effects of solvent consumption will overestimate LLI due to SEI but underestimate LAM if electrolyte dry-out occurs. Adding sufficient extra electrolyte into cells during manufacturing can greatly improve the capacity retention (~7% in our case) compared with those without any extra electrolyte

Solvent consumption and electrolyte dry-out.—The degradation behaviour of cells with different initial extra electrolytes is affected by the solvent consumption process and the resulting electrolyte dry-out. Figure 4 shows the accumulated volume of EC consumption, the resulting EC concentration and SEI interfacial current density. A full description of these processes can be found in Appendix.

Similar to the LLI in Fig. 3b, the accumulated EC consumed volume in Fig. 4a increases even more slowly with cycle number. Both cells with 6% and 9% more electrolyte consume ~1.55 ml EC, while the cell with 0% more electrolyte consumes 1.45 ml EC after 1170 cycles. However, the EC concentrations in all three cells are almost identical, reducing significantly by 85% (from 4541 mol·l^{-1} to 686 mol·l^{-1}). Accordingly, the SEI interfacial current density of the three cells also overlap and decrease by 98% (from 3.5×10^{-4} A·m^{-2} to 6.69×10^{-6} A·m^{-2}). This decrease of SEI interfacial current density is due to the decreased EC concentration and thickened SEI layer, as presented in Eq. 4. Notably, the cell without
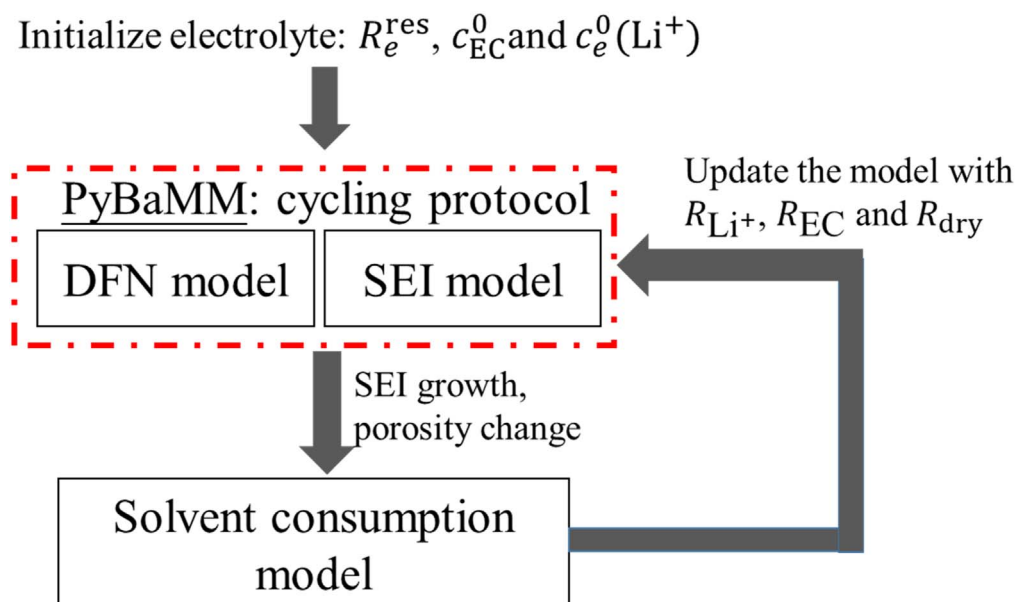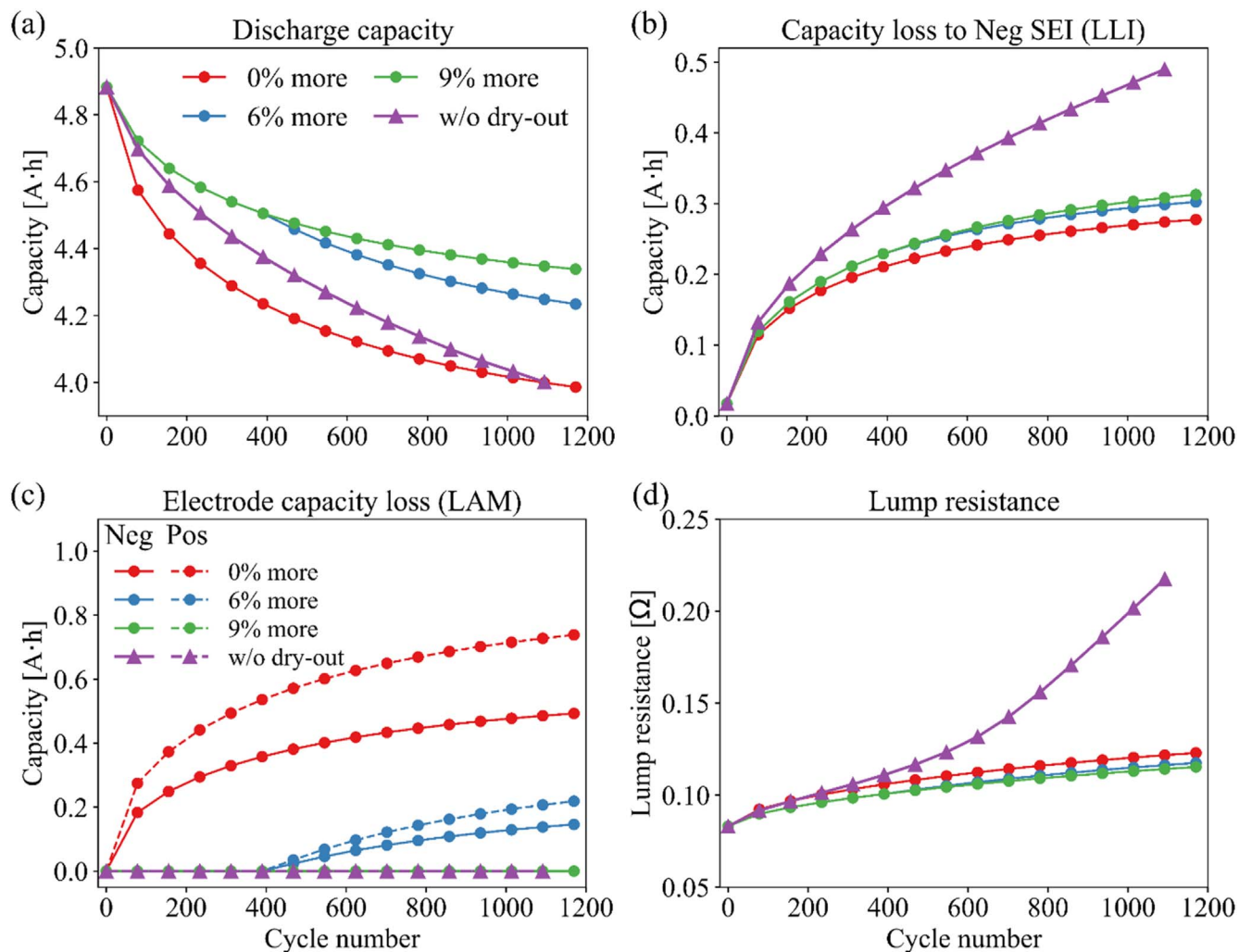

Figure 2. Model implementation through updating the simulation.

Figure 3. Degradation behaviour of cells with (circle) and without (triangle) the solvent consumption model: (a) C/10 discharge capacity at each RPT cycle; (b) capacity loss to negative electrode SEI; (c) electrode capacity loss at negative and positive electrode; (d) equivalent circuit model (ECM) resistance at end of C/10 discharge capacity, $R_{ECM} = (OCV - V_{terminal})/I$.

solvent consumption displays higher SEI interfacial current density during both the first and last ageing cycles, which can be attributed to the constant EC concentration. This explains the different LLI due to SEI of these cells in Fig. 3b.

Effects of solvent consumption on electrolyte properties.—The different rates in SEI growth (Fig. 4c) will lead to different negative electrode porosities, as presented in Figs. 5a and 5d. The negative electrode porosities of the three cells with solvent consumption reduce from 0.222 for the first ageing cycle to about ~0.123 for the last ageing cycle, whereas the porosity of the cell without solvent consumption decreases to 0.048. The extremely low negative electrode porosity leads to extreme lithium concentration in the electrolyte of the aged negative electrode, approaching zero at the end of the 0.3C constant current charge (Fig. 5b) and 6000 mol·m^{-3} at the end of 1C discharge (Fig. 5c). Even though we have not found any solubility limit of LiPF$_6$ in the electrolyte of this cell, (1 M LiPF$_6$ in EC/EMC 3:7 vol% with 1 wt% VC according to Chen et al.[31]), there is some evidence[36,37] indicating that such high concentration can lead to salt precipitation in commercial electrolytes for LIBs. Moreover, too high or too low lithium concentration makes the transport properties worse, as will be discussed later.

The large electrolyte concentration gradient will also lead to significant gradient in electrolyte potential, as presented in Figs. 5c and 5f. Overall, the electrolyte potential of the three cells with

solvent consumption increases at the end of 0.3C constant current charge and decreases at the end of 1C discharge after degradation. Such changes are more prominent in the cell without solvent consumption, with the electrolyte potential vs Li/Li$^+$ reaching +0.05 V near the negative electrode-separator interface at the end of 0.3C charge and −1.15 V at the end of 1C discharge. Note that in Ref. 5 which models the degradation induced by both SEI growth and lithium plating, an negative electrode porosity lower than 0.05 is regarded as pore clogging and is accompanied by the steep lithium concentration gradient and high electrolyte potential near the negative electrode-separator interface, which ultimately results in the accelerated lithium plating and sharp capacity drop.

The low porosity and high lithium concentration gradient in electrolyte give rise to larger gradients in interfacial current density in the negative electrodes, as presented in Fig. 6. The interfacial current density and reaction overpotential have small gradients in the first ageing cycle for all the cells. In the last ageing cycle, however, all the cells have large gradients of these two quantities across the negative electrode thickness. Cells with less initial extra electrolyte have a similar interfacial current density profile as those with more extra electrolyte but shift to a higher absolute value during both charge and discharge. This is because cells with less initial extra electrolyte have more severe LAM and therefore fewer active electrode particles to sustain the same externally applied current. A similar shift also occurs in the reaction overpotential of the negative electrode.
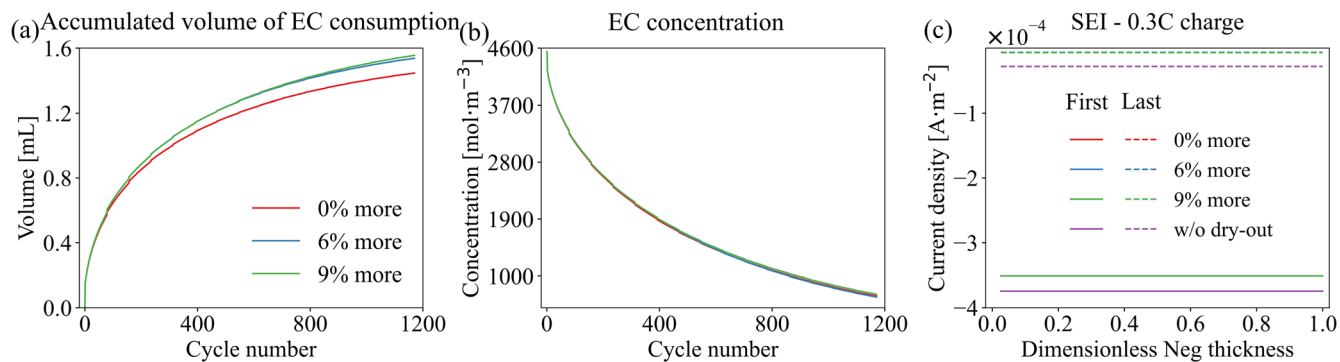
Figure 4. (a) Accumulated EC consumed volume of cells with different initial extra electrolyte volume; (b) EC concentration; (c) SEI interfacial current density at the end of the 0.3C constant current charge of the first (solid lines) and last (dashed lines) ageing cycles.
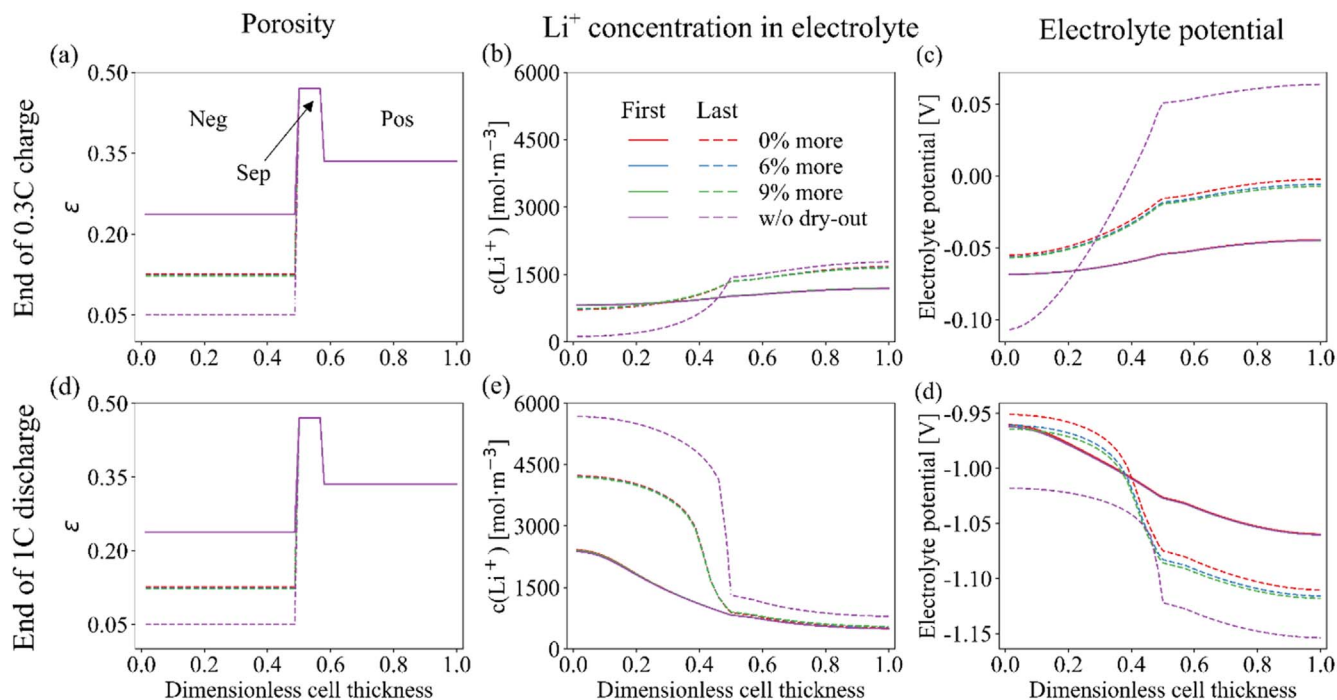
Figure 5. Effect on (a), (d) porosity, (b), (e) concentration, and (c), (f) electrolyte potential during the first and last ageing cycles. Panels (a)–(c) refer to the end of the 0.3C constant current charge, (d)–(f) refer to the end of the 1C discharge.

The cell without solvent consumption has even larger gradients in interfacial current density during both the end of charge and discharge, with the highest average absolute value. This means the interfacial current density can become higher due to lower porosity and smaller active electrode area. In practical applications, higher absolute values of the interfacial current density are likely to induce overcharge or over-discharge in particles, leading to other degradation mechanisms such as particle cracking and lithium plating.[11,38]

The steep concentration gradients and low porosity shown in Fig. 5 will reduce the effective electrolyte conductivity and diffusivity, which is defined as

$$D_{e,k}^{\text{eff}} = \varepsilon_k^b D_e(c_{e,k}) \qquad [33\text{-}1]$$

$$\sigma_{e,k}^{\text{eff}} = \varepsilon_k^b \sigma_e(c_{e,k}) \qquad [34]$$

where b is the Bruggeman coefficient. The standard assumption that $b = 1.5$ is applied in this work, which will amplify the effects of low porosity on the effective transport properties. As presented in Fig. 7, all the curves in the four sub-figures showed three distinguished regions corresponding to the negative electrode, the

separator, and the positive electrode, indicating that the effective transport properties are dominated by the porosity. At the end of 0.3C charge, all aged cells display lower effective electrolyte conductivity compared with the new ones. The three cells with solvent consumption overlap together, reducing from 0.1 S·m^{-1} to ~0.04 S·m^{-1} in the negative electrode, whereas the cell without solvent consumption has a conductivity approaching zero at the negative current collector. Similar results can be observed for the effective electrolyte diffusivity.

For the end of 1C discharge, both fresh and aged cells showed flat regions of the effective electrolyte conductivity and diffusivity near the negative current collector. This is because the equations (Eqs. A·3 and A·4) describing the electrolyte properties as a function of lithium concentration obtained from Nyman et al.[39] are only valid for $0 \sim 2000$ mol·m^{-3}. However, the lithium concentration in electrolyte exceeds 2000 mol·m^{-3} at the end of 1C discharge even for fresh cells. Further extrapolating the equations to a lithium concentration of up to 6000 mol·m^{-3} will lead to sharp increases of the conductivity and diffusivity (Fig. A·1), which is unrealistic.[40] Therefore, we have extrapolated the equations using the value at 2000 mol·m^{-3}, so that any changes in the effective electrolyte
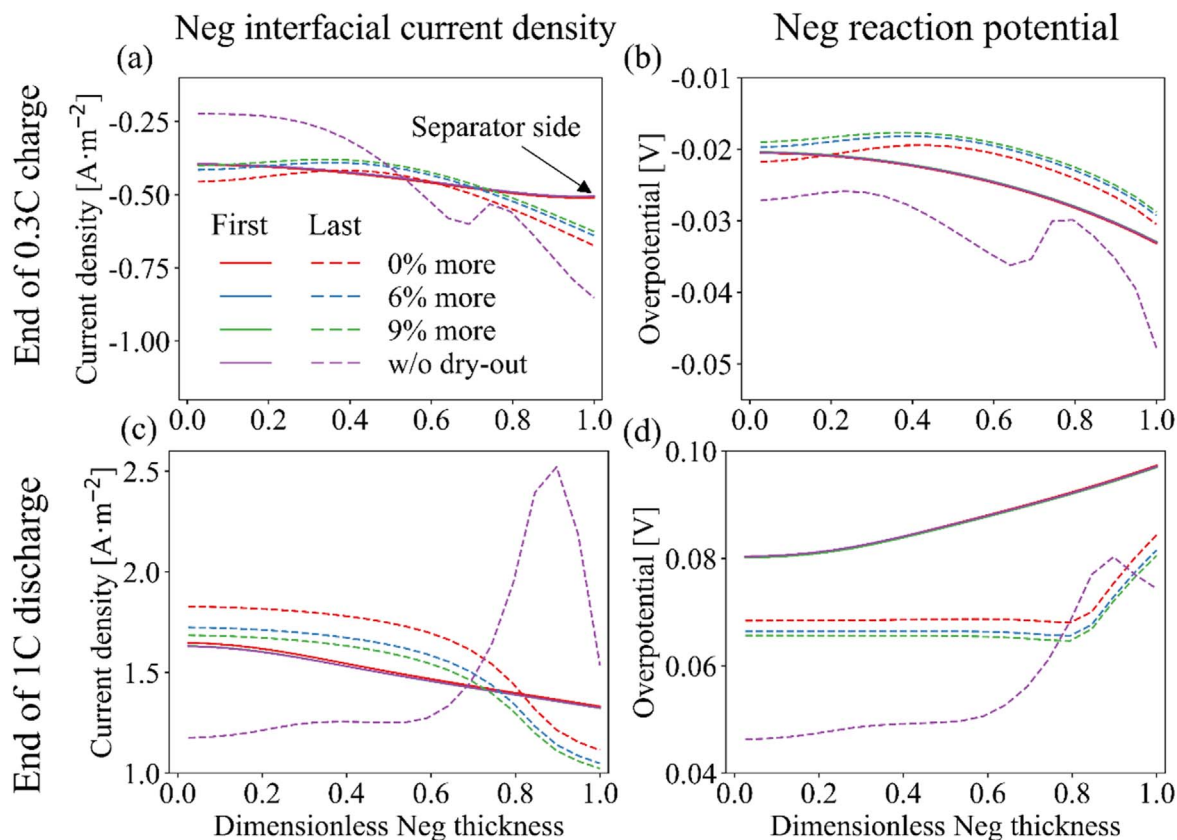
Figure 6. Effect on the (a), (c) negative interfacial current density for lithium intercalation, and (b), (d) negative SEI interfacial current density during the first and last ageing cycles. Panels (a)–(b) refer to the end of the 0.3C constant current charge, (c)–(d) refer to the end of the 1C discharge.

conductivity and diffusivity would be due to porosity changes. Nevertheless, the effective electrolyte conductivity and diffusivity of aged cells decrease significantly at the end of 1C discharge, with the lowest value occurring at the negative electrode due to the porosity reduction.

In summary, both the effective conductivity and diffusivity approaches zero at aged negative electrodes. That means the transport of lithium ions is very difficult here and requires much higher electrolyte potential gradient, as presented in Figs. 5c and 5f. The bad electrolyte transport properties together with the thicker SEI layers in cells without solvent consumption explains the sharp increase of local ECM resistance in Fig. 3d. The overpotential η_{Li} for the lithium plating reaction is given by[15]

$$\eta_{Li} = \phi_{s,n} - \phi_{e,n} - U_{Li} - \eta_{SEI} \qquad [34\text{-}1]$$

where U_{Li} is the equilibrium potential of lithium plating reaction and is set to 0 V. Based on Eq. 34, if the electrolyte potential becomes positive, η_{Li} is more likely to become negative, which increases the risk of lithium plating.

Conclusions

To deepen the understanding of SEI growth driven degradation of LIBs and increase the accuracy of battery life models, we incorporate a novel solvent consumption model into the standard DFN battery model. The solvent consumption model distinguishes the electrolyte volume fractions and porosities of battery components and considers the electrolyte volume as an independent variable.

We first derive the equations describing the solvent consumption based on the well-known EC-based SEI growth reaction. Our solvent consumption model is incorporated with the DFN model and solvent diffusion-limited SEI growth model in PyBaMM. The solvent consumption model influences the other two models directly through three aspects: changing the electrode area when dry-out occurs, changing the concentration of lithium ions and changing the concentration of solvent (in our case, EC). To save computational time, we implement such influences by updating the model parameters with three ratios within a certain frequency, without changing the core of PyBaMM.

To reveal the effects of solvent consumption, we compare the degradation behaviour of cells without solvent consumption and with solvent consumption but different initial electrolyte volume. We find that cells without solvent consumption will overestimate the LLI due to SEI but underestimate the LAM. For cells with solvent consumption, the cell with 9% initial extra electrolyte can retain 7% more capacity at the end of the ageing cycles compared with the cell with 0% initial extra electrolyte. These different degradation behaviours are caused by the interplay between two competing effects. On the one hand, solvent consumption may induce electrolyte dry-out, making part of the electrode materials inaccessible and therefore inducing LAM. On the other hand, the consumption of solvent reduces its concentration and therefore decreases the SEI interfacial current density, leading to less LLI due to SEI.

The solvent consumption also significantly influences the negative electrode porosity, the lithium-ion concentration in the electrolyte, the electrolyte potential, and the electrolyte transport properties. For the model not considering solvent consumption, more SEI growth led to much lower negative electrode porosity after ageing, leading to higher lithium-ion concentration and electrolyte potential gradients, causing the electrolyte potential at the negative electrode-separator interface to become positive. Moreover, the combined effects of lower porosities and extremely high or extremely low lithium concentration remarkably reduce the effective electrolyte
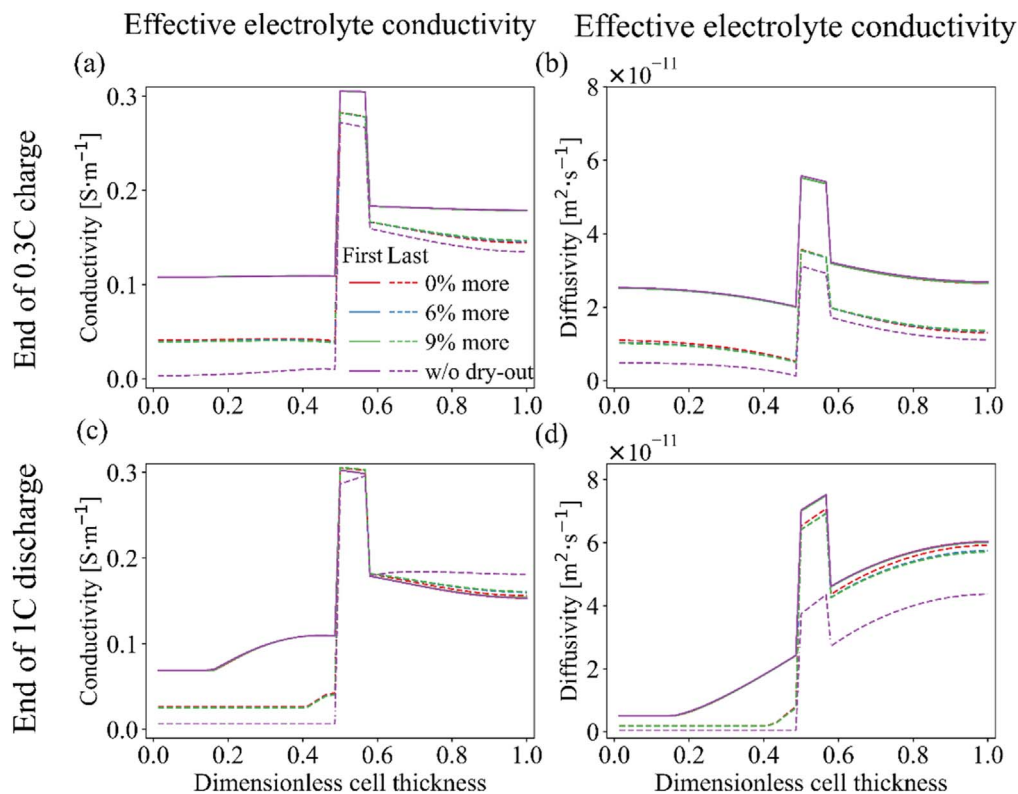
Figure 7. Effect on the (a, c) effective electrolyte conductivity, and (b, d) effective electrolyte diffusivity. Panels (a)–(b) refer to the end of the 0.3C constant current charge, (c)–(d) refer to the end of the 1C discharge.

conductivity and diffusivity. These changes may trigger lithium plating, given that previous studies have pointed out one possible cause for lithium plating is extremely low local negative electrode porosity.

The interplay between solvent consumption and SEI growth may produce a positive feedback loop due to LAM and higher interfacial current density, but negative feedback is also possible due to the reduced solvent (in our case, EC) concentration. The diffusion-limited SEI growth mechanism assumed in this study is only weakly affected by interfacial current density, causing the negative feedback to dominate in this work. Note that the model in this work is developed assuming only EC is consumed, but the model can be easily applied to other EC-free electrolytes as well. Future work will focus on discussing the interactions between solvent consumption, SEI growth, lithium plating and other battery degradation mechanisms.

From an engineering perspective, the most significant conclusion is that the model predicts that it should be possible to significantly increase cell lifetime by adding extra electrolyte to keep the active region wetted throughout its life. This is currently a qualitative prediction, but once parameterised and validated for a given cell, the model has the potential to be used as a design tool to optimise the electrolyte amount necessary to avoid cell dry-out triggered LAM.

Author statement

Ruihe Li: Writing—original draft, review & editing; Simon O'Kane: Review & editing; Monica Marinescu: Funding acquisition, supervision; Gregory J Offer: Funding acquisition, supervision, review & editing.

Appendix

Model parameters.—In Fig. A·1, "initial" means that the electrolyte properties are calculated from Eq. A·3 and Eq. A·4, which comes from Ref. 39 and only applicable for a concentration range of no more than 2M. Further extrapolating these two equations to a high lithium-ion concentration of up to 6M will produce unreasonable results. Therefore, we have used the constant extrapolation for lithium-ion concentrations higher than 2M in the simulation for the sake of simplicity.

Description of electrolyte dry-out.—The three ratios in Figs. A·3d∼A·3f mean the ratio of electrolyte dry-out, lithium ions concentration change, and EC concentration change, respectively. These three ratios are calculated based on Eqs. 26, 30, and 32, respectively.

Check sensitivity of update frequency.—In this study, we implement our solvent consumption model by updating the cell through three ratios. This assumes that the solvent consumption is a slow process that only have considerable effects in the long term, such as dozens of ageing cycles. Here we will check sensitivity of the results on this update frequency and consolidate our assumption. Specifically, we run the cell with 6% initial extra electrolyte with the same ageing conditions but different update frequencies.

In Figs. A·2 and A·3, the capacity loss, LLI, electrode capacity, lump resistance, and voltage are almost the same regardless of the frequencies we chose, consolidating our assumption that the solvent consumption is a slow process, and the update method can simulate electrolyte dry-out accurately with little increase in computational resources.

Table A·I. The parameter used for the DFN model in this study (otherwise specially stated, all parameters are from Chen et al.[31]).

Type	Parameter	Unit	Positive electrode	Separator	Negative electrode
	Active material		$LiNi_{1-x-y}Mn_xCo_yO_2$	Ceramic coated polyolefin	Graphite + silicon
Design specifications	Current collector thickness	m	$1.6 \cdot 10^{-5}$		$1.2 \cdot 10^{-5}$
	Electrode thickness (L_k)	m	$7.56 \cdot 10^{-5}$	$1.2 \cdot 10^{-5}$	$8.52 \cdot 10^{-5}$
	Electrode length	m	1.58		
	Electrode width	m	$6.5 \cdot 10^{-2}$		
	Mean particle radius (R_k)	m	$5.22 \cdot 10^{-6}$		$5.86 \cdot 10^{-6}$
	Electrolyte volume fraction (ε_k)		0.335	0.47	0.25
	Active material volume fraction ($\varepsilon_{s,k}$)		0.665		0.75
	Bruggeman exponent (b)		1.5	1.5	1.5
Electrode	Solid phase lithium diffusivity ($D_{s,k}$)	$m^2 \cdot s^{-1}$	$1.48 \cdot 10^{-15}$		$1.74 \cdot 10^{-15}$
	Solid phase electronic conductivity ($\sigma_{s,k}$)	$S \cdot m^{-1}$	0.18		215
	Maximum concentration ($c_{s,k}^{max}$)	$mol \cdot m^{-3}$	63104		33133
	Stoichiometry at 0% SOC		0.8331^e		0.02906^e
	Stoichiometry at 100% SOC		0.2700^e		0.8728^e
Electrolyte	Electrolyte ionic diffusivity ($D_{e,k}$)	$m^2 \cdot s^{-1}$		Fig. A·1a or Eq. A·3	
	Electrolyte ionic conductivity ($\sigma_{e,k}$)	$S \cdot m^{-1}$		Fig. A·1b or Eq. A·4	
	Transference number (t^+)			0.2594	
	Initial electrolyte concentration ($c_{e,0}$)	$mol \cdot m^{-3}$		1000	
Intercalation reaction	Open Circuit Voltages (U_k)	V	Fig. A·2b or Eq. A·1		Fig. A·2b or Eq. A·2
	Activation energy	$J \cdot mol^{-1}$	17800		35000
	Reaction rate (m_k)	$A \cdot m^{-2} \cdot (m^3 \cdot mol^{-1})^{1.5}$	$3.42 \cdot 10^{-6}$		$6.48 \cdot 10^{-7}$

e: estimated from parameter fitting

$$U_p^{eq} = -0.8090 \cdot y + 4.4875$$
$$-0.0428 \cdot \tanh(18.5138 \cdot (y - 0.5542))$$
$$-17.7326 \cdot \tanh(15.7890 \cdot (y - 0.3117))$$
$$+17.5842 \cdot \tanh(15.9308 \cdot (y - 0.3120)) \quad \text{[A·1]}$$

$$U_n^{eq} = 1.9793 \cdot e^{-39.3631 \cdot x} + 0.2482$$
$$-0.0909 \cdot \tanh(29.8538 \cdot (x - 0.1234))$$
$$-0.04478 \cdot \tanh(14.9159 \cdot (x - 0.2769))$$
$$-0.0205 \cdot \tanh(30.4444 \cdot (x - 0.6103)) \quad \text{[A·2]}$$

$$D_{e,k} = 8.794 \cdot 10^{-17} \cdot c_{e,k}^2 - 3.972 \cdot 10^{-13} \cdot c_{e,k} + 4.862 \cdot 10^{-10} \quad \text{[A·3]}$$

$$\sigma_{e,k} = 1.297 \cdot 10^{-10} \cdot c_{e,k}^3 - 2.51 \cdot 10^{-4.5} \cdot c_{e,k}^{1.5} + 3.329 \cdot 10^{-3} \cdot c_{e,k} \quad \text{[A·4]}$$
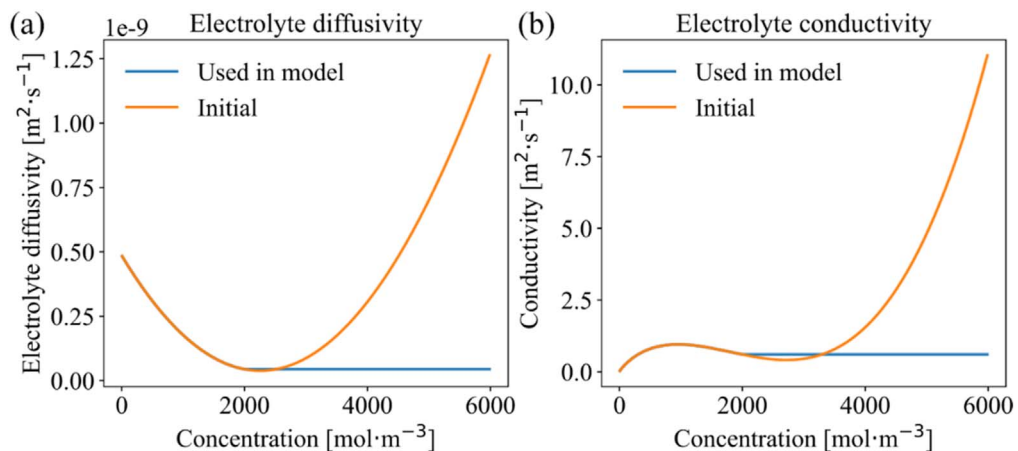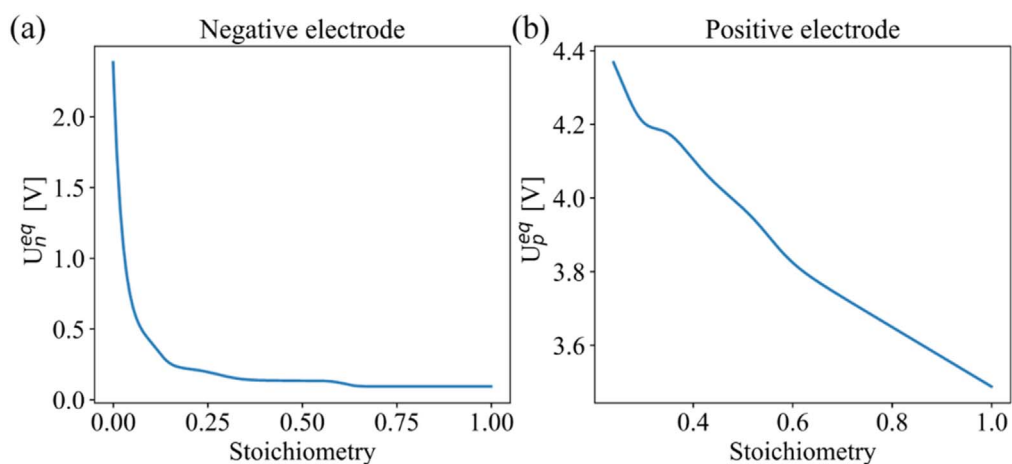
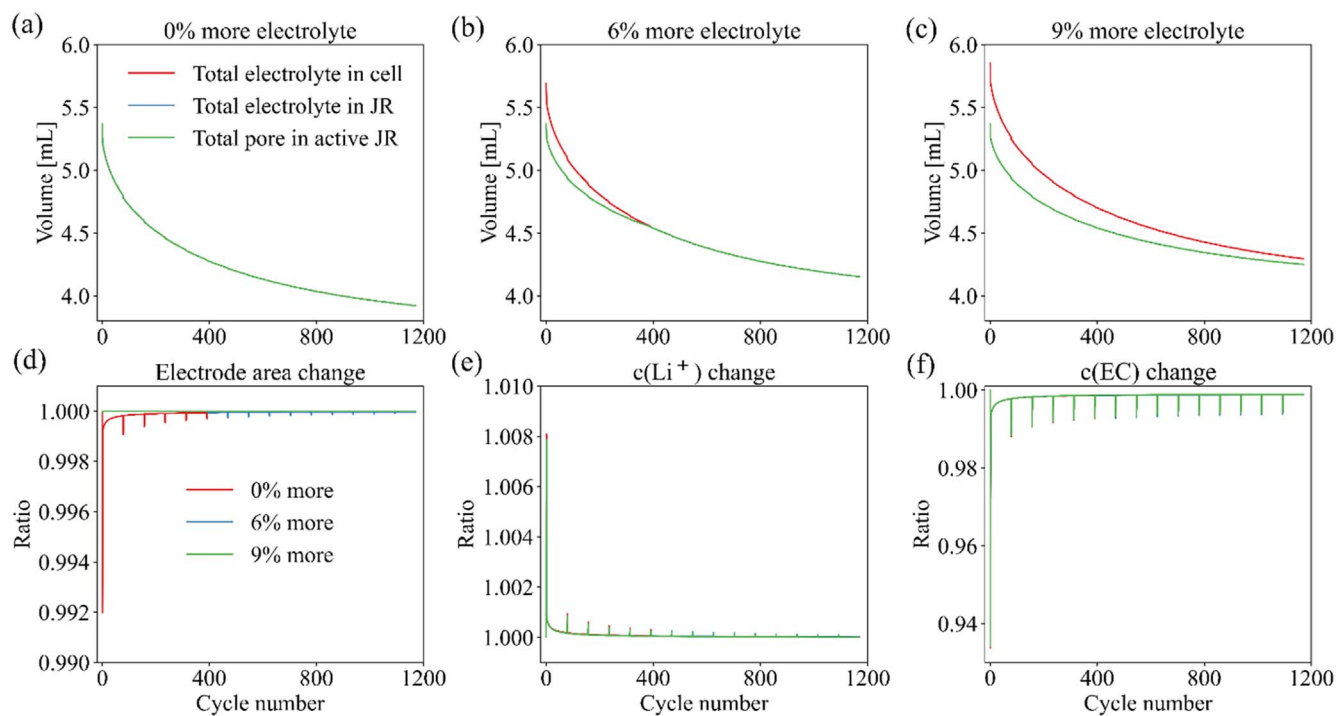**Figure A·1.** Electrolyte properties
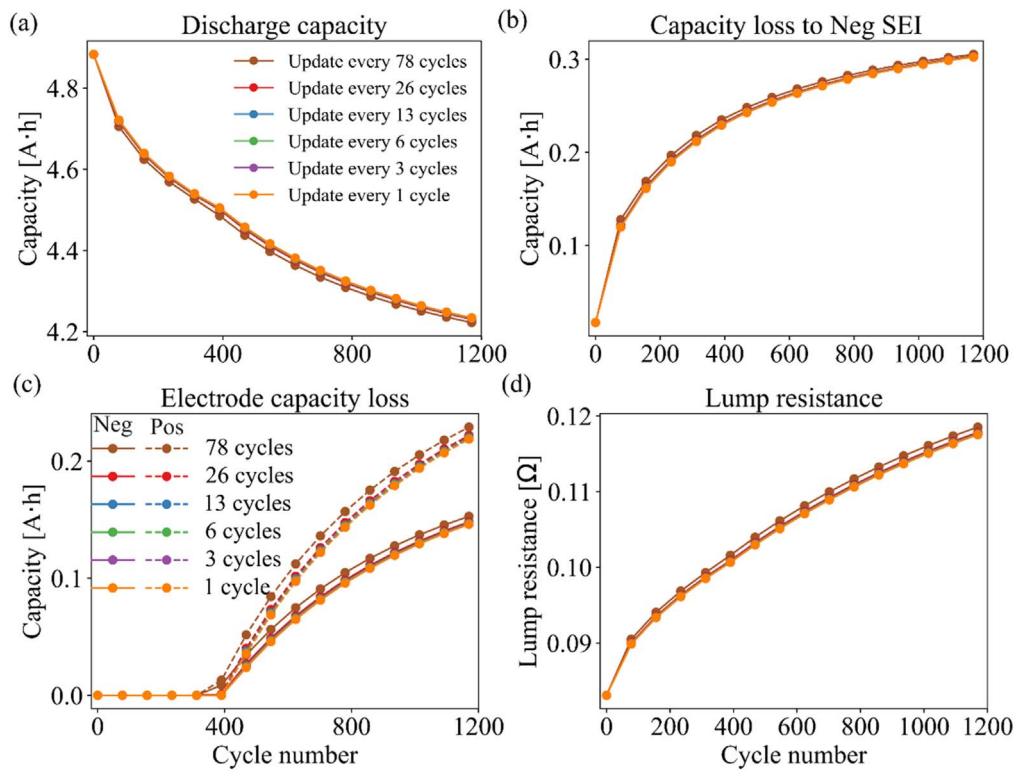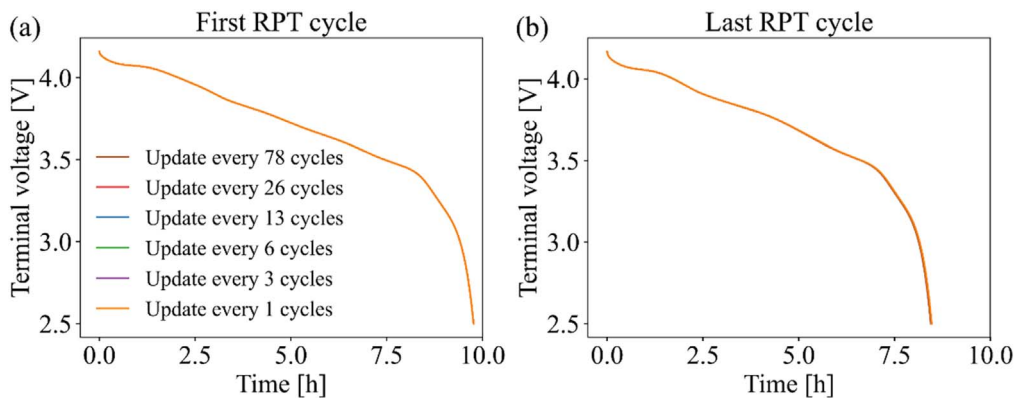

Figure A·2. Electrode OCV

Figure A·3. (a)–(c) Electrolyte and pore volume change with different initial extra electrolyte volume; ratio of (d) electrolyte dry-out; (e) lithium-ion concentration change; (f) EC concentration change.

Figure A·4. Degradation behaviour for different update frequencies (6% more electrolyte)

Figure A·5. Terminal voltage at first and last RPT cycles for different update frequencies (6% more electrolyte).

Table A·II. The parameter used for the SEI and solvent consumption model.

| Parameter	Unit	Value
Inner SEI reaction proportion (α)		0.5
Inner SEI partial molar volume	m^3·mol^{-1}	$9.585\cdot10^{-5}$
Outer SEI partial molar volume	m^3·mol^{-1}	$9.585\cdot10^{-5}$
SEI conductivity (σ_{SEI})	S·m^{-1}	$5\cdot10^{-6}$
Initial EC concentration (c_{EC}^0)	mol·m^{-3}	4541
Initial inner SEI thickness ($\delta_{SEI,inn}^0$)	m	$2.5\cdot10^{-9}$
Initial outer SEI thickness ($\delta_{SEI,out}^0$)	m	$2.5\cdot10^{-9}$
EC diffusivity through the outer SEI ($D_{EC}^{SEI,out}$)	m^2·s^{-1}	$1.7\cdot10^{-20}$
Ratio of initial extra electrolyte		0, 6%, 9%
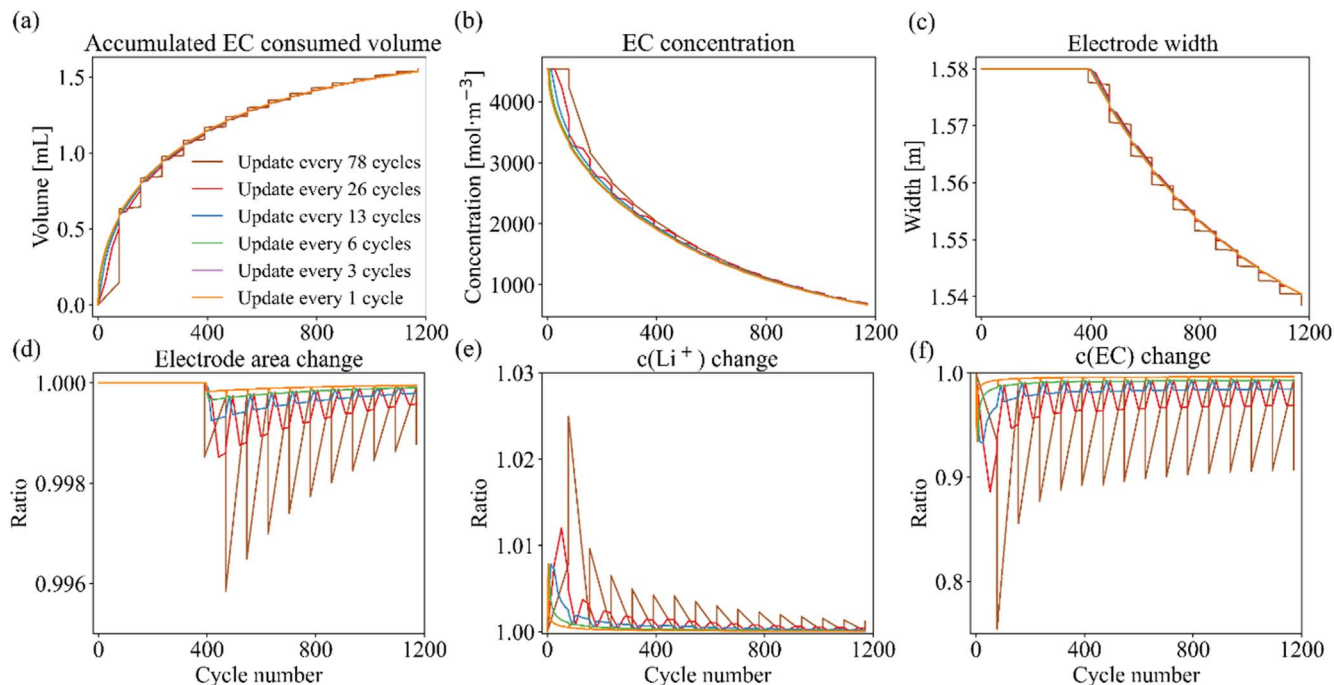
Figure A·6. Description of electrolyte dry-out for different update frequencies (6% more electrolyte.)

ORCID

Ruihe Li https://orcid.org/0000-0003-0965-8952
Simon O'Kane https://orcid.org/0000-0003-3141-1657
Monica Marinescu https://orcid.org/0000-0003-1641-3371
Gregory J Offer https://orcid.org/0000-0003-1324-8366

References

1. C. R. Birkl, M. R. Roberts, E. McTurk, P. G. Bruce, and D. A. Howey, *J. Power Sources*, **341**, 373 (2017).
2. M. Safari, M. Morcrette, A. Teyssot, and C. Delacourt, *J. Electrochem. Soc.*, **156**, A145 (2009).
3. S. G. Marquis, *Thesis*, University of Oxford (2020), (http://epg.eng.ox.ac.uk/content/degradation-lithium-ion-batteries).
4. S. Atalay, M. Sheikh, A. Mariani, Y. Merla, E. Bower, and W. D. Widanage, *J. Power Sources*, **478**, 229026 (2020).
5. X. G. Yang, Y. Leng, G. Zhang, S. Ge, and C. Y. Wang, *J. Power Sources*, **360**, 28 (2017).
6. X. Lin, J. Park, L. Liu, Y. Lee, A. M. Sastry, and W. Lu, *J. Electrochem. Soc.*, **160**, A1701 (2013).
7. F. M. Kindermann, J. Keil, A. Frank, and A. Jossen, *J. Electrochem. Soc.*, **164**, E287 (2017).
8. R. D. Deshpande and D. M. Bernardi, *J. Electrochem. Soc.*, **164**, A461 (2017).
9. R. Deshpande, M. Verbrugge, Y. T. Cheng, J. Wang, and P. Liu, *J. Electrochem. Soc.*, **159**, 1730 (2012).
10. I. Laresgoiti, S. Käbitz, M. Ecker, and D. U. Sauer, *J. Power Sources*, **300**, 112 (2015).
11. J. Vetter, P. Novák, M. R. Wagner, C. Veit, K. C. Möller, J. O. Besenhard, M. Winter, M. Wohlfahrt-Mehrens, C. Vogler, and A. Hammouche, *J. Power Sources*, **147**, 269 (2005).
12. X. Han, L. Lu, Y. Zheng, X. Feng, Z. Li, J. Li, and M. Ouyang, *eTransportation*, **1**, 100005 (2019).
13. V. A. Agubra and J. W. Fergus, *J. Power Sources*, **268**, 153 (2014).
14. P. Verma, P. Maire, and P. Novák, *Electrochim. Acta*, **55**, 6332 (2010).
15. D. Ren, K. Smith, D. Guo, X. Han, X. Feng, L. Lu, M. Ouyang, and J. Li, *J. Electrochem. Soc.*, **165**, A2167 (2018).
16. P. Ramadass, B. Haran, P. M. Gomadam, R. White, and B. N. Popov, *J. Electrochem. Soc.*, **151**, A196 (2004).
17. F. Single, A. Latz, and B. Horstmann, *ChemSusChem*, **11**, 1950 (2018).
18. A. M. Colclasure, K. A. Smith, and R. J. Kee, *Electrochim. Acta*, **58**, 33 (2011).
19. T. R. Ashwin, Y. M. Chung, and J. Wang, *J. Power Sources*, **328**, 586 (2016).
20. J. Liu and C. W. Monroe, *Electrochim. Acta*, **167**, 357 (2015).
21. F. J. Günter, J. E. Soc, F. J. Günter, C. Burgstaller, F. Konwitschny, and G. Reinhart, *J. ofThe Electrochem. Soc.*, **166**, A1709 (2019).
22. R. LI, D. Ren, S. Wang, Y. Xie, Z. Hou, L. Lu, and M. Ouyang, *J. Energy Storage*, **40**, 102788 (2021).
23. B. P. Matadi et al., *J. Electrochem. Soc.*, **164**, A1089 (2017).
24. D. Ren et al., *eTransportation*, **2**, 100034 (2019).
25. J. Park, W. A. Appiah, S. Byun, D. Jin, M. H. Ryou, and Y. M. Lee, *J. Power Sources*, **365**, 257 (2017).
26. C. Kupper, B. Weißhar, S. Rißmann, and W. G. Bessler, *J. Electrochem. Soc.*, **165**, A3468 (2018).
27. R. Fang, P. Dong, H. Ge, J. Fu, Z. Li, and J. Zhang, *J. Energy Storage*, **42**, 103013 (2021).
28. M. Doyle, T. F. Fuller, and J. Newman, *J. Electrochem. Soc.*, **140**, 1526 (1993).
29. G. L. Plett, *Battery Management Systems, Volume I: Battery Modeling* (Artech House, Massachusetts, MA) (2015).
30. J. Newman and K. E. Thomas-Alyea, *Electrochemical Systems* (Wiley, New York, NY) (2012).
31. C.-H. Chen, F. Brosa Planella, K. O'Regan, D. Gastol, W. D. Widanage, and E. Kendrick, *J. Electrochem. Soc.*, **167**, 080534 (2020).
32. H. J. Ploehn, P. Ramadass, and R. E. White, *J. Electrochem. Soc.*, **151**, A456 (2004).
33. K. Xu, *Chem. Rev.*, **104**, 4303 (2004).
34. V. Sulzer, S. Marquis, R. Timms, M. Robinson, and S. J. Chapman, *J. Open Res. Softw.*, **9**, 14 (2021).
35. J. M. Reniers, G. Mulder, and D. A. Howey, *J. Electrochem. Soc.*, **166**, A3189 (2019).
36. L. O. Valøen and J. N. Reimers, *J. Electrochem. Soc.*, **152**, A882 (2005).
37. A. A. Wang, A. B. Gunnarsdóttir, J. Fawdon, M. Pasta, C. P. Grey, and C. W. Monroe, *ACS Energy Lett.*, **6**, 3086 (2021).
38. A. Tomaszewska et al., *eTransportation*, **1**, 100011 (2019).
39. A. Nyman, M. Behm, and G. Lindbergh, *Electrochim. Acta*, **53**, 6356 (2008).
40. J. Landesfeind and H. A. Gasteiger, *J. Electrochem. Soc.*, **166**, A3079 (2019).